

Safely assessing RF heating potential of conductive devices using image-based current measurements

Greg Griffin¹, Kevan Anderson², and Graham A Wright^{1,2}

¹Medical Biophysics, University of Toronto, Toronto, Ontario, Canada, ²Imaging Research, Sunnybrook Research Institute, Toronto, Ontario, Canada

Purpose: The purpose of this work was to demonstrate the feasibility of using MRI-based radiofrequency (RF) current measurements to predict RF heating in the vicinity of conductive structures undergoing MRI. Several clinically useful conductive devices pose RF safety risks when scanned during MRI. These include interventional/diagnostic catheters, deep brain stimulator leads, pacemaker leads, and cochlear implants to name a few. At present the RF heating potential of a certain device is investigated in a representative phantom by directly measuring temperature rise around a device; there currently exists no technique to safely assess the RF heating potential of a certain patient/device configuration *in situ* before applying a potentially dangerous scanning protocol. The presented technique attempts to safely assess induced RF current on a conductive device and predict heating behavior under sequences with higher power deposition.

Methods: This study was carried out using the ASTM F2182-11a standard heating phantom filled with saline doped poly-acrylic acid gel [1]. A plastic lighting louver with 1.5 cm square cells was used to fix ASTM recommended holders that supported the conductor and a fiber-optic (FO) temperature sensor during scanning. Scanning was performed using an Optima MR450W 1.5T scanner (GE, Milwaukee, USA). Four experiments are discussed here; all of which measured current on and heating near copper magnet wire (Belden, Indianapolis, USA) insulated along its length and bare at the tips. The first two experiments used partially immersed wires; mimicking a percutaneous intervention. In the first two experiments a 120cm length of wire with approximately 28 cm immersed, oriented parallel to the scanner bore and held at the approximate location (x,y)=(12cm,-9cm) with the distal tip at z=0 was scanned. The first two experiments used AWG 24 and AWG 26 wire respectively. The third and fourth experiments used 25cm wires fully immersed in phantom gel, mimicking an implanted medical device. AWG 24 and AWG 26 wires were again used and held in the same axial position, this time with the center of the wires at z=0. In all experiments, a FO temperature sensor (OpSens, QC, Canada) was held parallel to the wire at a distance of 1.8mm using a custom holder. The wire and FO tips were aligned with no offset in the longitudinal direction.

Each experiment employed the same workflow. Several axial gradient-echo (GRE) images (TE/TR=min full/18ms, FA=10, BW=15.63kHz, 256x256, NEX=12, FOV=24cm, Slice=0.5cm) were acquired along the length of each wire, to provide a single measurement of RF current at the location of each image. 13 GRE images were acquired in each experiment, with no spacing between images, covering the distal 6cm of each wire. A fast spin-echo (FSE) sequence (TE/TR=14/425ms, Echo Train=4, BW=15.63kHz, 256x256, NEX=5, FOV=40cm, Slice=1cm, Scan Time=16m5s) similar to the ASTM recommended heating sequence was then applied as a representative sequence with high specific absorption rate (SAR), approximately 21 times that of the GRE sequence used. Temperature reported by the FO sensor was recorded throughout all measurement and heating scans.

Each RF current value was extracted using a previously described technique [2]. The low-resolution current distribution produced by this analysis was then up-sampled using cubic spline interpolation to a resolution of 0.25mm. From this high-resolution current distribution the resultant magnetic vector potential and subsequently SAR distribution were calculated in a 40x40x40 cube of side length 2 cm centered on the tip of the wire at which heating was being measured. The resultant SAR distribution was then normalized to the average power of the heating sequence and using a Green's function solution to Pennes' bioheat equation [3], the temperature evolution and predicted steady-state distribution were calculated on the same grid as SAR.

Results: No measurable temperature rise was recorded during any current measurement scans. Presented in Figure 1 are measured and predicted temperature rises in Kelvin as seen during application of the heating scan. In all plots, an uncertainty inherent to the holder of 0.5mm in the position of the FO sensor is represented; the lower blue line represents the predicted temperature rise for the closest potential position (0.25mm closer than expected) and the upper blue line that for the farthest.

Discussion: In all plots it can be seen that the theoretical temperature rise agrees well with the measured temperature rise. The goal of this study was to present a technique that can safely assess RF heating potential. Heating experiment 3 produced a temperature rise that would certainly be dangerous to a patient, however no dangerous temperature rise was recorded during current measurement. This is a result of the relatively low RF power deposition of the GRE sequence. The low flip-angle and absence of refocusing 180° RF pulses in the GRE sequence allow for images to be acquired with much lower RF energy deposition. Specifically, the SAR of the FSE sequence was approximately 21 times that of the GRE sequence, resulting in a temperature rise approximately 21 times greater when applying the FSE sequence as compared to the GRE sequence. This factor allows for safe assessment of potentially very dangerous conditions, and the safety of the GRE measurement sequence could easily be increased by increasing TR. The results shown report a temperature rise as a function of time to enable good visualization of the results. To calculate this temperature evolution is a computationally intensive procedure, as a 3D convolution must be performed for each time point. In a practical setting however only the steady-state temperature distribution would be required to identify unsafe conditions thus reducing computation time (one 3D convolution) to <1s on a typical modern laptop computer.

Conclusion: In its present form, this study demonstrates the feasibility of this technique to safely predict unsafe RF conditions during MRI scanning. *In vivo* however, many factors such as local susceptibility differences; chemical shift and gradient non-linearities near the bore wall could potentially reduce the accuracy of measurements. Simulation work is ongoing to show that an ultra-short echo time gradient echo sequence can be used to overcome typical errors associated with the aforementioned factors. Other future work includes investigating conductive structures with arbitrary geometry.

References: [1] ASTM Standard F2182-11a [2] Griffin G. et al. ISMRM 2012;30:2727 [3] Yeung et al. Med. Phys. 2001;25:826

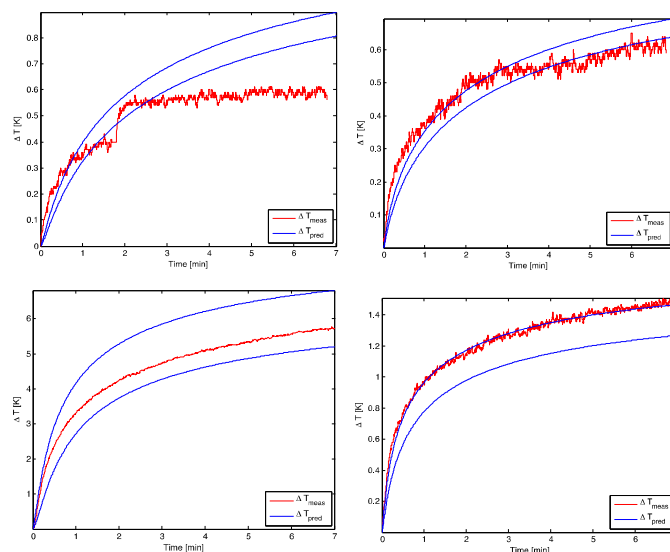


Figure 1(a-d): Measured and theoretical temperature rise as calculated using MRI-based current measurements. The left column shows results for the AWG 26 wire, and the right column results for the AWG 24 wire. The top row is experiments mimicking intervention and the bottom experiments mimicking implanted devices. For clarity, all time axes run from 0-7min.